

# Effects of sea level rise on salinity and tidal flooding patterns in the Guadiana Estuary

Lara Mills, João Janeiro and Flávio Martins

## ABSTRACT

Sea level rise is a worldwide concern as a high percentage of the population is located in coastal areas. The focus of this study is the impact of sea level rise in the Guadiana Estuary, an estuary in the Iberian Peninsula formed at the interface of the Guadiana River and the Gulf of Cadiz. Estuaries will be impacted by sea level rise as these transitional environments host highly diverse and complex marine ecosystems. The major consequences of sea level rise are the intrusion of salt from the sea into fresh water and an increase in flooding area. As the physical, chemical, and biological components of estuaries are sensitive to changes in salinity, the purpose of this study is to further evaluate salt intrusion in the Guadiana Estuary caused by sea level rise. Hydrodynamics of the Guadiana Estuary were simulated in a two-dimensional numerical model with the MOHID water modeling system. A previously developed hydrodynamic model was implemented to further examine changes in salinity distribution in the estuary in response to sea level rise. Varying tidal amplitudes, freshwater discharge from the Guadiana River and bathymetries of the estuary were incorporated in the model to fully evaluate the impacts of sea level rise on salinity distribution and flooding areas of the estuary. Results show an overall increase in salinity and land inundation in the estuary in response to sea level rise.

**Key words** | Guadiana Estuary, numerical model, sea level rise

**Lara Mills** (corresponding author)

**João Janeiro**

**Flávio Martins**

Centro de Investigação Marinha e Ambiental (CIMA),

University of Algarve,

Faro,

Portugal

E-mail: [lkrm347@gmail.com](mailto:lkrm347@gmail.com)

**Flávio Martins**

Instituto Superior de Engenharia (ISE), University of Algarve,

Faro,

Portugal

## HIGHLIGHTS

- Implementation of a numerical model to evaluate changes in the hydrodynamics of the Guadiana Estuary due to sea level rise.
- Production of salinity distribution maps for the Guadiana Estuary in response to climate change.
- An analysis of the hydrodynamics of the estuary based on varying freshwater flow rates, tidal amplitudes, and sea level rise scenarios.
- Understanding how estuarine dynamics change along different bathymetries.

This is an Open Access article distributed under the terms of the Creative Commons Attribution Licence (CC BY-NC-ND 4.0), which permits copying and redistribution for non-commercial purposes with no derivatives, provided the original work is properly cited (<http://creativecommons.org/licenses/by-nc-nd/4.0/>).

doi: 10.2166/wcc.2021.202

## INTRODUCTION

### Sea level change

Global mean sea level is rising at a rate of approximately 3.2 millimeters per year (Church *et al.* 2013). According to the most recent report from the Intergovernmental Panel on Climate Change (IPCC), the rate of global mean sea level rise has been increasing over the last two centuries and continues to accelerate. Sea level rise will affect coastal areas, which should be a concern considering 10% of the world's population live within 10 m elevation of the present sea level (Carrasco *et al.* 2016). Direct consequences of sea level rise on coastal areas include an increase in flooding area, an increase in erosion, and an increase in salinity and changes in ecosystems (Nicholls *et al.* 2011). Of relevance to the present study is the impact of sea level rise on estuaries, where rivers intersect sea and freshwater mixes with saltwater.

### Effects of sea level rise on estuaries

Salt intrusion is a direct consequence of sea level rise in estuaries (McLean *et al.* 2001). Estuarine circulation is mainly driven by freshwater flow, tides, and density differences (Garel *et al.* 2009). A study by Chua & Xu (2014) found a stronger longitudinal salinity gradient in estuaries due to sea level rise, which in turn drives a stronger gravitational circulation. The increase in salinity will cause the water to become denser, and thus increase the stratification of the water column. Changes in estuarine stratification and circulation will further cause oxygen depletion (Hong & Shen 2012). These effects are detrimental to ecosystem services and marine habitat as estuaries hold highly diverse and complex ecosystems (Sampath *et al.* 2015). The objective of this study is to evaluate the evolution of hydrodynamics and changes in salinity distribution in response to various sea level rise scenarios in a major estuary in the Iberian Peninsula, the Guadiana Estuary.

### Physical characteristics of the Guadiana Estuary

The Guadiana Estuary is formed at the interface of the Guadiana River and the Gulf of Cadiz. The head of the Guadiana River begins in Spain and extends 810 km south

toward the Gulf of Cadiz (Delgado *et al.* 2012). From its mouth in front of Vila Real de Santo António, the Guadiana Estuary extends 80 km north to its tidal limit near Mértola, Portugal. Because of its narrow width and moderate depth, the Guadiana Estuary is considered a rock-bound estuary where the volume of water entering the estuary during the flood tide is larger than the freshwater discharge (Garel & D'Alimonte 2017). Tidal and riverine processes are the dominant forces in the estuary and the action of the waves is considered negligible (Garel *et al.* 2009). The Guadiana Estuary is characterized by a semidiurnal mesotidal regime (Sampath & Boski 2016) with an average neap tidal range of 1.28 m and an average spring tidal range of 2.56 m (Garel *et al.* 2009). The western margin of the estuary is characterized by a salt marsh sheltered by a littoral sand spit that drains into the estuarine channel (Garel *et al.* 2009). The eastern margin is composed of barrier islands and sand spits separated by extensive salt marshes that drain to the Gulf of Cadiz through a tidal inlet (Garel *et al.* 2009). The flow rate from the Guadiana River varies drastically from less than 10 to 4,660 m<sup>3</sup>/s. The construction of over 100 dams for water storage and irrigation since the 1950s has strongly reduced the freshwater flow rate (Garel *et al.* 2009). Of importance is the Alqueva Dam located 60 km upstream of the head of the estuary (Garel & D'Alimonte 2017). This large reservoir was completed in 2002 and since then the freshwater flow into the estuary has been reduced from a yearly average of 143 to 16 m<sup>3</sup>/s (Garel *et al.* 2009). The reduction in flow rate also has an impact on residence time, the time it takes a particle to exit the system (Oliveira *et al.* 2006). The residence time of salinity for a river discharge of 8 m<sup>3</sup>/s ranges between 6 and 60 days, but when the river flow is high, the residence time ranges from a few hours to 9 days (Oliveira *et al.* 2006). Thus, the discharge of the Guadiana River has a large effect on the horizontal distribution of salinity in the estuary. The Guadiana Estuary is well-mixed when the freshwater discharge from the Guadiana River is low and is partially stratified for higher discharges. When there is a higher tidal amplitude and lower discharge from the Guadiana River, tidal processes control the water circulation of

the estuary and the estuary becomes well-mixed (Garel & D'Alimonte 2017). The estuary is weakly stratified when it is neap tide and the river discharge is low (Garel & D'Alimonte 2017). In the latter case, density-driven processes control the mixing of the estuary. The water column is stratified only under extreme conditions (Basos 2013).

## METHODS

### MOHID

Hydrodynamics and water properties of the Guadiana Estuary were simulated with the Modelo Hidrodinâmico (MOHID, hereafter) water modeling system in response to different scenarios of sea level rise. MOHID is programmed in ANSI FORTRAN 95 in order to produce object-oriented models integrating hydrodynamic processes for different marine systems (MARETEC 2017). The present study used a two-dimensional model in MOHID, as the Guadiana Estuary is classified as a well-mixed estuary (Garel & D'Alimonte 2017), meaning that the water column is vertically homogeneous. The Guadiana Estuary can become stratified, but only under freshwater flows of  $1,000 \text{ m}^3/\text{s}$  (Fortunato *et al.* 2002). The present study ran simulations for freshwater flows of 10 and  $100 \text{ m}^3/\text{s}$  as these are typical conditions of the system after the closure of the Alqueva Dam. This further justifies the use of a two-dimensional model, allowing for long (1–2 month) simulations, which would have had prohibitive computational costs with a three-dimensional model. MOHID solves Navier–Stokes equations with the hydrostatic approximation, using the finite volume method over a generic geometric grid. In this work, hydrodynamic and Eulerian transport modules were used. The finite volume method allows for the transport equations to be applied to the entire cell volume at specific points in discrete time (Neves *et al.* 2000). Of relevance are the results of a study by Mills *et al.* (2019) as the present study builds upon the methodologies used to simulate hydrodynamics and changes in salinity distribution with respect to sea level rise. These authors used MOHID in two dimensions (2D, hereafter) to simulate the hydrodynamics of the Guadiana Estuary considering different sea level rise

scenarios up to the year 2100 along with varying freshwater flow rates of the Guadiana River (Mills *et al.* 2019). Results of the model demonstrated an overall increase in salinity in the estuary as well as flooding area around the estuary with respect to sea level rise. Sea level rise led to a reduction in water velocity in the main channel, most likely due to an increase in depth and water volume (Mills *et al.* 2019). The model considered only the present bathymetry as well as a tidal amplitude equivalent to the average tidal amplitudes. The horizontal distribution of salinity in estuaries is dependent on several factors. One major variable is the balance between spring and neap tidal cycles and freshwater flow (Vargas *et al.* 2017). It is, thus, the aim of this work to expand upon the methodologies of Mills *et al.* (2019) to determine how the horizontal distribution of salinity varies between spring and neap tide as well as across a bathymetry that will allow flooding of the surrounding marshes.

### Model setup

The present study implements the same general setup of the model by Mills *et al.* (2019) and uses the same Cartesian computational grid of  $1,400 \times 350$  cells with a resolution of 30 m. This computational mesh was chosen as it provides the most appropriate spatial resolution without incurring excessive calculation time. The calculation time for each simulation is high, especially when the river discharge is low. Two months of simulation time is required due to the high residence time when the freshwater flow rate is low (Oliveira *et al.* 2006). The hydrodynamic MOHID model of the Guadiana Estuary has been previously validated, calibrated, and used in several studies (Lopes *et al.* 2003; Morais *et al.* 2012). The present model consists of two separate bathymetries: (1) a bathymetry in which coastal management strategies are implemented to keep the coastline as it is (Figure 1) and (2) a bathymetry that allows for geomorphological changes caused by sea level rise and thus allows flooding around the estuary (Figure 2). The future state of the bathymetry of the Guadiana Estuary could fall anywhere between these two extremes, and thus, the present paper aims to analyze the differences between an unchanged coastline and a coastline that allows flooding. The first bathymetry is the current bathymetry of the

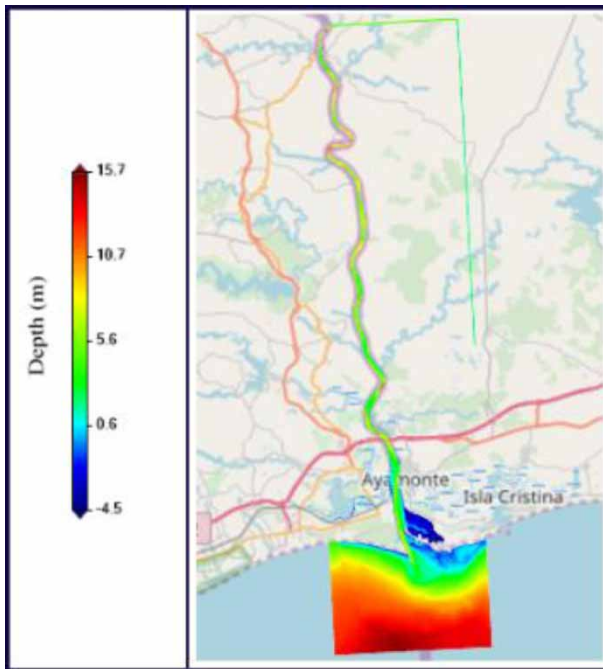


**Figure 1** | Bathymetry of the Guadiana Estuary corresponding to a maintained coastline on a mesh of  $1,400 \times 350$  cells with a resolution of 30 m (Mills *et al.* 2019).

Guadiana Estuary and was computed by triangular interpolation of measured bathymetric data on the Cartesian grid of  $1,400 \times 350$  cells (Mills *et al.* 2019). The second bathymetry was computed by Sampath *et al.* (2011) in a behavior-oriented model. This bathymetry allows the surrounding saltmarshes and low-lying areas of the estuary to be flooded. It was solved based on the rate of sea level change, accommodation space for the deposition of sediments, and vertical accretion of sediments dependent on inundation (Sampath *et al.* 2011).

Various sea level rise cases were chosen based on future sea level rise projections from the 5th assessment report by the IPCC. The 5th assessment report includes sea level rise forecasts up to the year 2100 for different Representative Concentration Pathways (RCP), more commonly known as greenhouse gas emissions (Church *et al.* 2013). The study by Mills *et al.* (2019) considered values forecasted by the IPCC for a case of low greenhouse gas emissions (RCP 4.5) and a case of very high greenhouse gas emissions (RCP 8.5). Values were chosen based on the average predictions for the years 2045–2065, 2081–2100, and 2100 for both RCP values. The values imposed in the model include a sea level rise of 0.24 m for 2040, 0.48 m for 2070, and 0.79 m for

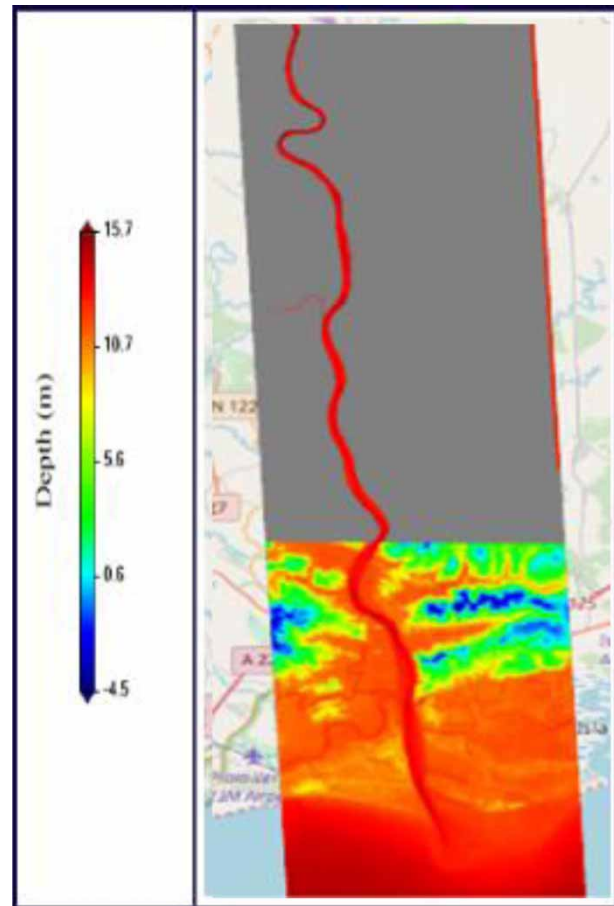


**Figure 2** | Bathymetry of the Guadiana Estuary corresponding to an unmaintained coastline ( $1,400 \times 350$  cells with a resolution of 30 m). The gray space is land (Sampath *et al.* 2011).

2100. Two freshwater flow scenarios were chosen based on typical annual conditions of the freshwater flow rate from the Guadiana River and include: (1) a low discharge of  $10 \text{ m}^3/\text{s}$  representing the summer months when there is little rain and (2) a high discharge of  $100 \text{ m}^3/\text{s}$  for the remaining months when there is more rainfall. These two values for river discharge are appropriate as the freshwater flow has been strongly regulated since the closure of the Alqueva Dam, yielding a reduction in the seasonal variability of the river discharge (Quesada *et al.* 2019). Two tidal amplitudes were imposed in the model to examine how the dynamics of the estuary vary at spring tide and neap tide. Since this study did not aim at representing a specific period, a simple M2 tide was imposed. The amplitudes representing spring and neap tides are 1.28 and 0.64 m, respectively.

## Areas of inundation

Areas of inundation were computed for the various scenarios of sea level rise and highest freshwater discharge scenario ( $100 \text{ m}^3/\text{s}$ ) over the bathymetry allowing flooding. The methodologies follow those of Mills *et al.* (2019) who computed flooding area as a function of the number of hours of land submersion during one tidal cycle, but only for a freshwater discharge of  $500 \text{ m}^3/\text{s}$ . The present study includes an analysis of flooding area for a river discharge of  $100 \text{ m}^3/\text{s}$  as well as each spring and neap tide scenario. Ten classes of flooding were computed as a function of submersion time over 1 tidal cycle (12.5 h). For example, class 1 corresponds to a submersion time of 0–1.2 h, class 2 corresponds to a submersion time of 1.2–2.4 h, and so forth. Histograms and flood distribution maps were computed based on the percentage of time a land cell was covered by water in the grid during one tidal cycle.

## RESULTS

### Time series locations

Time series graphs of water velocity, water elevation, and salinity were produced along with several locations of the

estuary. The locations and nomenclature used for the time series analysis are shown in Figure 3.

### Temporal evolution of salinity

Time series graphs were produced at each location shown in Figure 3, allowing for an assessment of the evolution of salinity over two tidal cycles (approximately 24.48 h) for each sea level rise scenario. The average change in salinity every 30 years is summarized in Tables 1 and 2. The simulations for salinity distribution assume a salinity value of 0 for freshwater and a value of 36 for seawater.

### Horizontal distribution of salinity

The following section examines the horizontal distribution of salinity along with water velocity direction at a time instant 1 h before high tide. As can be seen in the time series results, changes in salinity throughout the scenarios of sea level rise vary for the present bathymetry, whereas results from the alternate bathymetry reveal a correlation between sea level rise and salinity. Thus, all horizontal distribution maps of salinity are shown for the present bathymetry, whereas only the present year compared with 2100 are shown for the bathymetry allowing flooding.

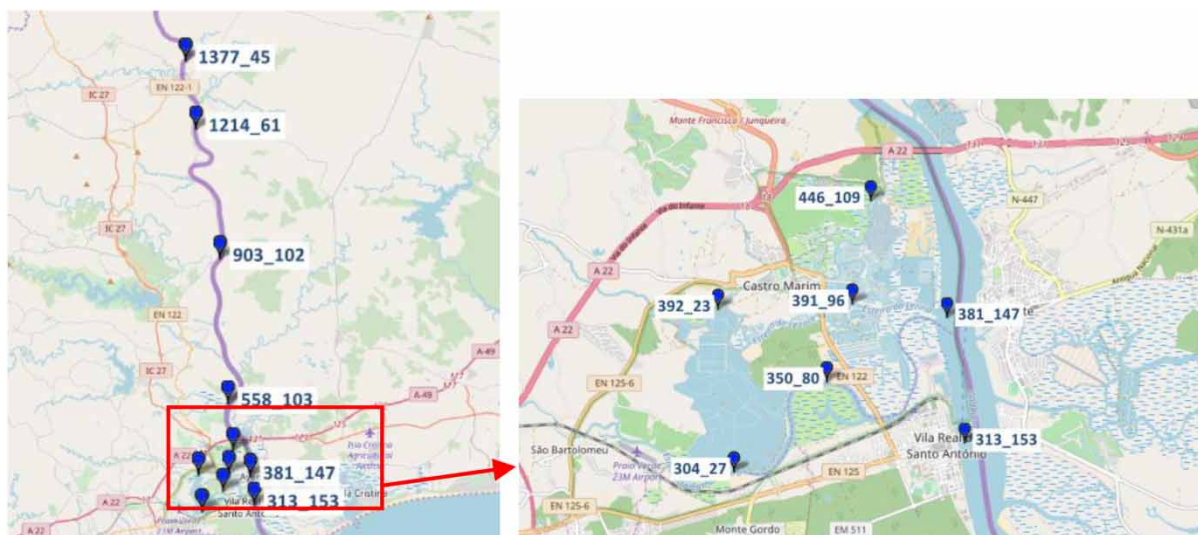


**Figure 3** | Location and nomenclature for points used in the time series along the main channel (left) and saltmarshes (right).

**Table 1** | Change in salinity for a discharge of 100 m<sup>3</sup>/s at neap tide and spring tide

		Change in salinity											
		Neap tide						Spring tide					
		Present bathymetry			Flooding bathymetry			Present bathymetry			Flooding bathymetry		
Estuary location		Present-2040	2040-2070	2070-2100	Present-2040	2040-2070	2070-2100	Present-2040	2040-2070	2070-2100	Present-2040	2040-2070	2070-2100
Upper	1377_45	0.000	0.000	0.000	0.000	0.000	0.000	0.000	0.000	0.000	0.000	0.000	0.000
	1214_61	0.000	0.000	0.000	0.000	0.000	0.000	0.000	0.000	0.000	0.000	0.000	0.000
Middle	903_102	0.000	0.000	0.000	0.000	0.000	0.056	0.000	0.000	0.000	0.000	0.000	0.000
	558_103	0.000	0.000	0.000	0.005	0.014	0.032	0.050	0.012	0.002	0.710	0.921	1.058
Lower	381_147	-0.051	-0.053	-0.028	1.030	1.191	1.494	0.380	0.083	0.121	1.236	1.409	1.540
	313_153	0.063	0.046	0.127	1.098	1.195	1.437	0.584	0.174	0.271	1.286	1.341	1.432
Marshes	446_109	-0.010	0.003	0.025	0.369	0.718	0.901	-0.151	-0.235	-0.184	2.041	1.805	2.125
	392_23	-0.008	0.008	0.042	0.255	0.550	0.565	-0.152	-0.239	-0.186	1.233	1.720	2.038
	391_96	-0.013	-0.005	0.006	0.492	0.768	0.989	-0.432	-0.609	-0.416	1.590	1.709	1.995
	350_80	-0.124	-0.049	-0.013	0.190	0.437	0.766	-0.970	-1.191	-0.928	1.321	1.661	1.974
	304_27	-0.148	-0.049	-0.002	0.176	0.410	0.710	-1.119	-1.272	-0.915	0.766	1.151	1.631

**Table 2** | Change in salinity for a discharge of 10 m<sup>3</sup>/s at neap tide and spring tide

		Change in salinity											
		Neap tide						Spring tide					
		Present bathymetry			Flooding bathymetry			Present bathymetry			Flooding bathymetry		
Estuary location		Present-2040	2040-2070	2070-2100	Present-2040	2040-2070	2070-2100	Present-2040	2040-2070	2070-2100	Present-2040	2040-2070	2070-2100
Upper	1377_45	0.000	0.000	0.001	0.000	0.000	0.000	-0.001	0.000	0.002	0.001	0.002	0.002
	1214_61	-0.001	0.003	0.009	0.001	0.002	0.002	-0.008	0.003	0.017	0.010	0.013	0.018
Middle	903_102	-0.170	0.344	0.375	0.081	0.106	0.138	-0.342	0.114	0.547	0.311	0.360	0.527
	558_103	-6.993	9.093	0.136	1.025	1.288	1.414	-2.378	0.037	2.020	1.739	1.636	2.494
Lower	381_147	-3.422	3.435	1.321	1.072	1.174	0.966	-1.311	-0.212	1.114	1.061	0.784	1.165
	313_153	-1.869	1.885	1.143	0.649	0.653	0.507	-0.944	-0.096	0.774	0.606	0.482	0.777
Marshes	446_109	-3.822	3.459	2.773	1.685	1.571	0.524	-2.464	-0.460	1.368	2.201	0.834	1.409
	392_23	-3.834	3.075	2.959	0.839	1.821	-6.112	-2.287	-0.551	1.239	5.989	0.684	0.186
	391_96	-4.557	4.257	1.774	1.503	1.584	0.057	-2.287	-0.551	1.239	2.164	0.830	1.273
	350_80	-3.002	2.333	2.535	1.551	1.850	1.456	-2.199	-0.682	0.754	1.352	1.160	1.849
	304_27	-2.526	1.680	3.371	1.596	1.875	1.489	-2.228	-0.725	0.618	1.488	1.227	2.126

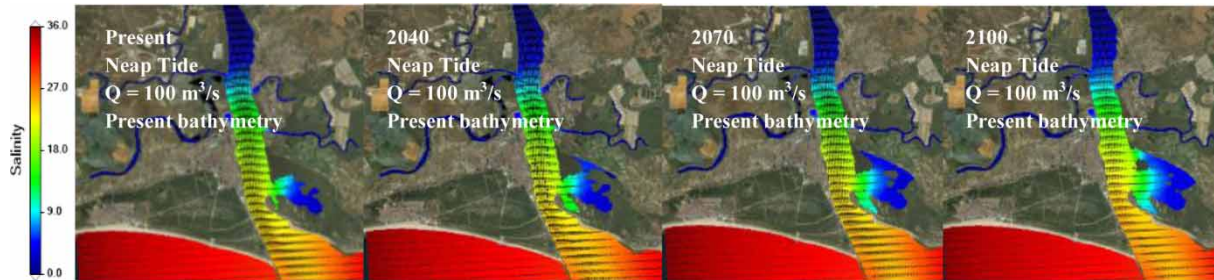


**Figure 4** | Water velocity direction and salinity distribution for a high freshwater flow at neap tide for the present bathymetry for each scenario of sea level rise 1 h before high tide.

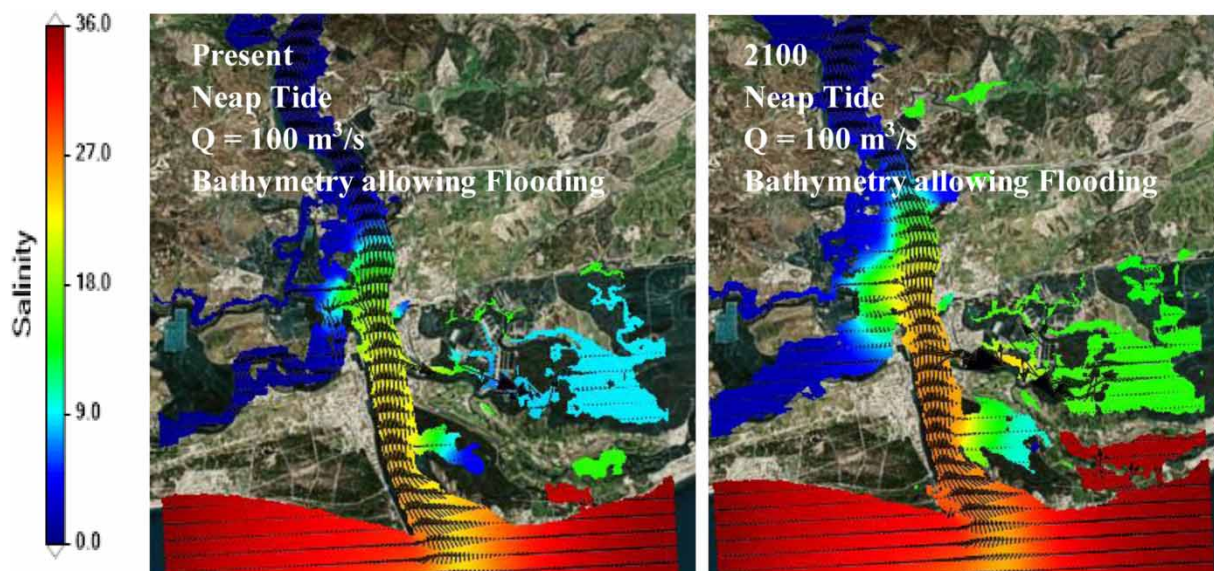


**Figure 5** | Water velocity direction and salinity distribution for a high freshwater flow at neap tide for the bathymetry allowing flooding 1 h before high tide.

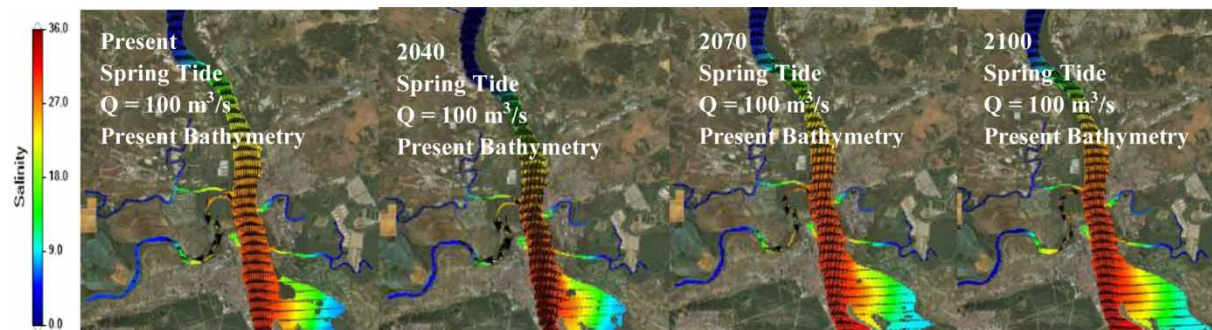


**Figure 6** | Water velocity direction and salinity distribution for a high freshwater flow at spring tide for the present bathymetry 1 h before high tide.

### High freshwater discharge at neap tide

See Figures 4 and 5.

### High freshwater discharge at spring tide

See Figures 6 and 7.

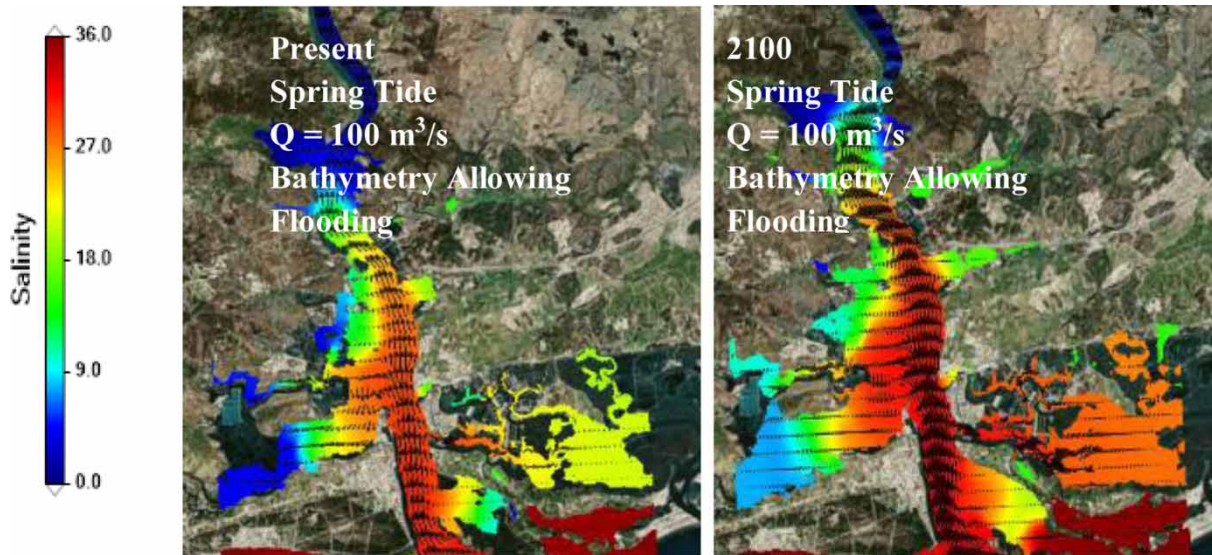


**Figure 7** | Water velocity direction and salinity distribution for a high freshwater flow at spring tide for the bathymetry allowing flooding.

### Low freshwater discharge at neap tide

See [Figures 8 and 9](#).

### Salinity classes

Salinity classes were computed based on the amount of area covered by specific salinity values. A salinity class of 1 corresponds to salinity values between 0 and 5, a salinity class of 2 corresponds to salinity values between 5 and 10, and so forth. Salinity classes were computed for all tidal

scenarios and freshwater discharge scenarios to examine the differences between the present and 2100. The results are shown in [Figures 10 and 11](#).

### Low freshwater discharge at spring tide

See [Figures 12 and 13](#).

### Areas of flooding

See [Figures 14–17](#).

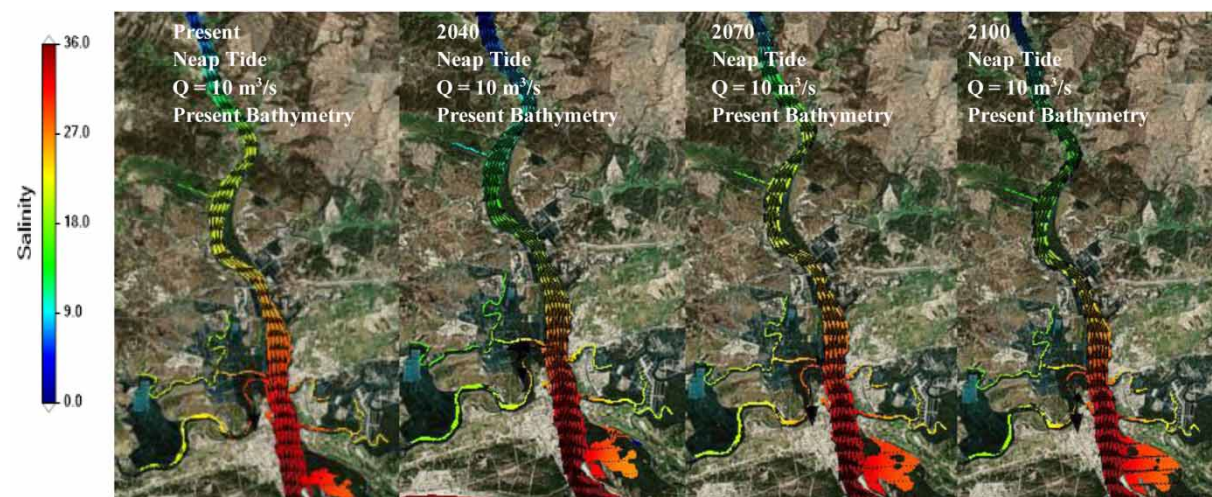


**Figure 8** | Water velocity direction and salinity distribution for a low freshwater flow at neap tide for the present bathymetry at a time instant of 1 h before high tide.

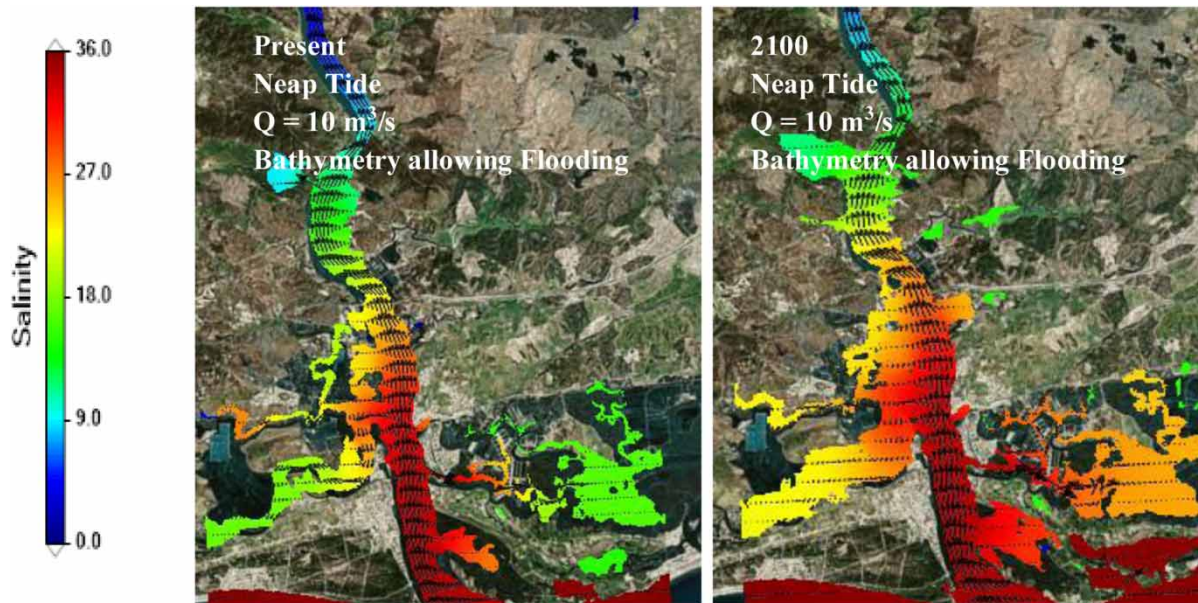


**Figure 9** | Water velocity direction and salinity distribution for a low freshwater flow at neap tide for the bathymetry allowing flooding 1 h before high tide.

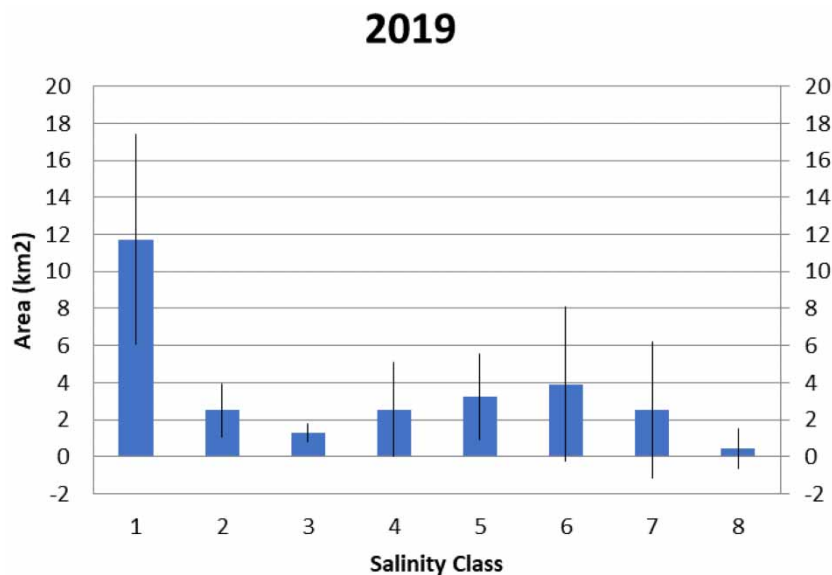


**Figure 10** | Salinity classes derived from all scenarios for the present.

## DISCUSSION

The results obtained from the MOHID model have shown the dynamics of the Guadiana Estuary to be complex, especially with respect to the tides. For the bathymetry allowing flooding, salinity increase is correlated to sea level rise for all cases of freshwater flow and for each tidal

scenario. On the other hand, the present bathymetry that does not allow the coastline to be changed results in a complex dynamic where salinity values vary at different locations with respect to sea level rise.

The horizontal distribution of salinity intrusion depends on the freshwater flow and tidal scenario. When the freshwater flow from the Guadiana River is high the marshes

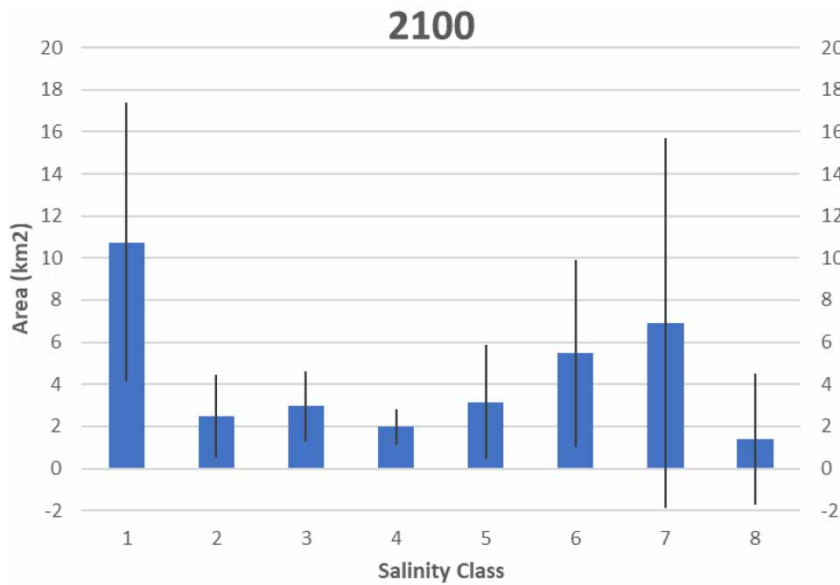


**Figure 11** | Salinity classes derived from all scenarios for 2100.

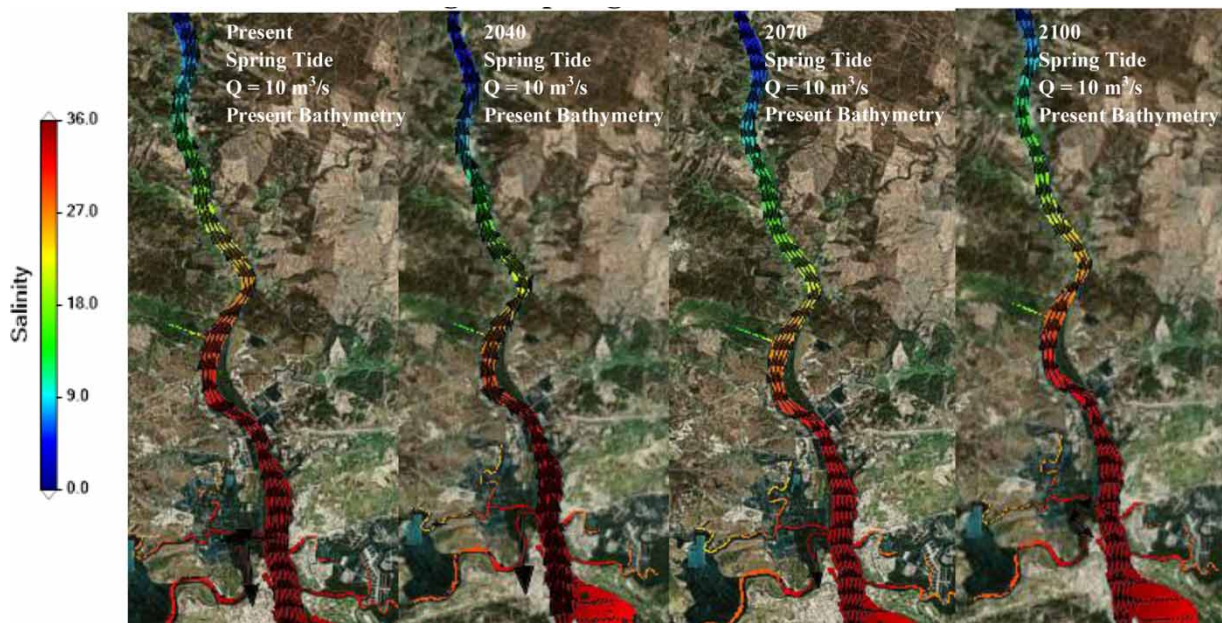


**Figure 12** | Water velocity direction and salinity distribution at all areas affected by the salinity front for a high freshwater flow at spring tide for the present bathymetry.

east and west of the Guadiana Estuary increase in salinity. Areas further upstream of the estuary portray an increase in salinity when the river discharge is low. These results are consistent with those from Mills *et al.* (2019) who also found larger changes in water velocity and salinity in the marshes near Esteiro da Leziria (381\_147) on the western

margin of the estuary for higher freshwater discharges compared with changes in water velocity and salinity in the main channel. Likewise, results from Mills *et al.* (2019) found larger changes in water velocity and salinity upstream of the main channel for low freshwater discharges. The bathymetry allowing flooding demonstrates increases in salinity

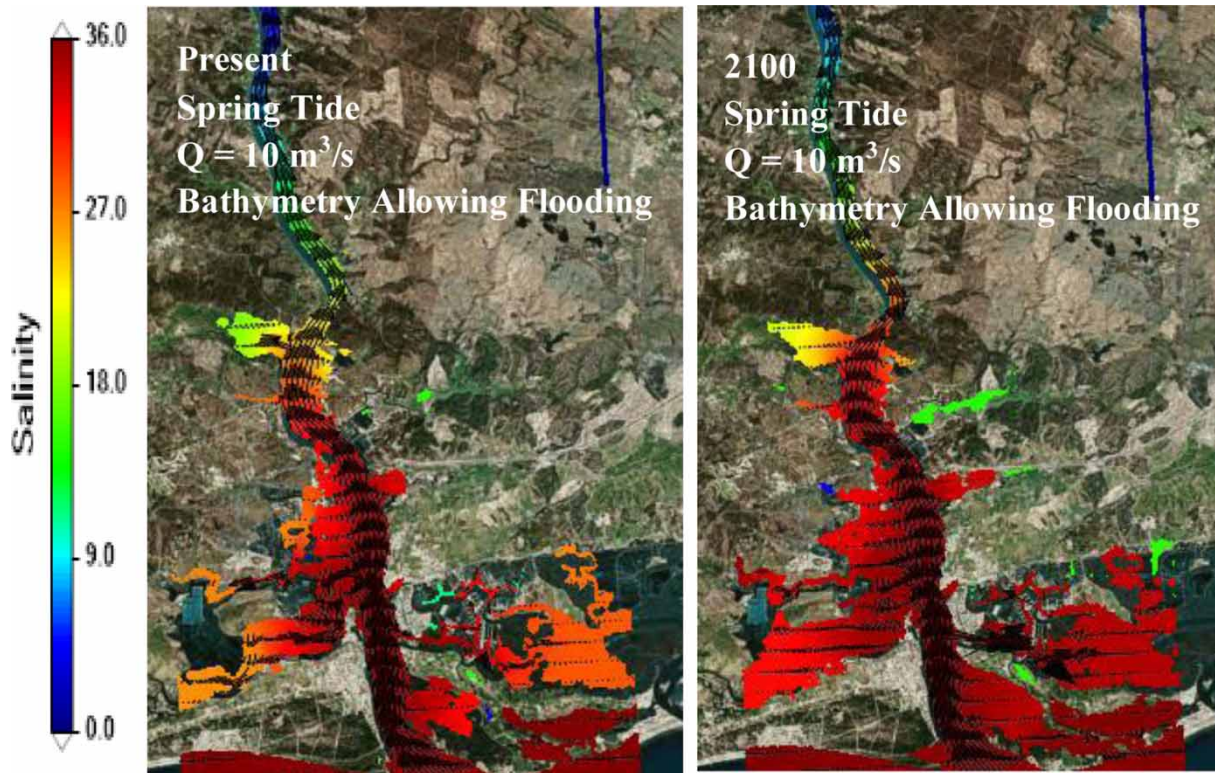


**Figure 13** | Water velocity direction and salinity distribution for a low freshwater flow at spring tide for the present bathymetry.

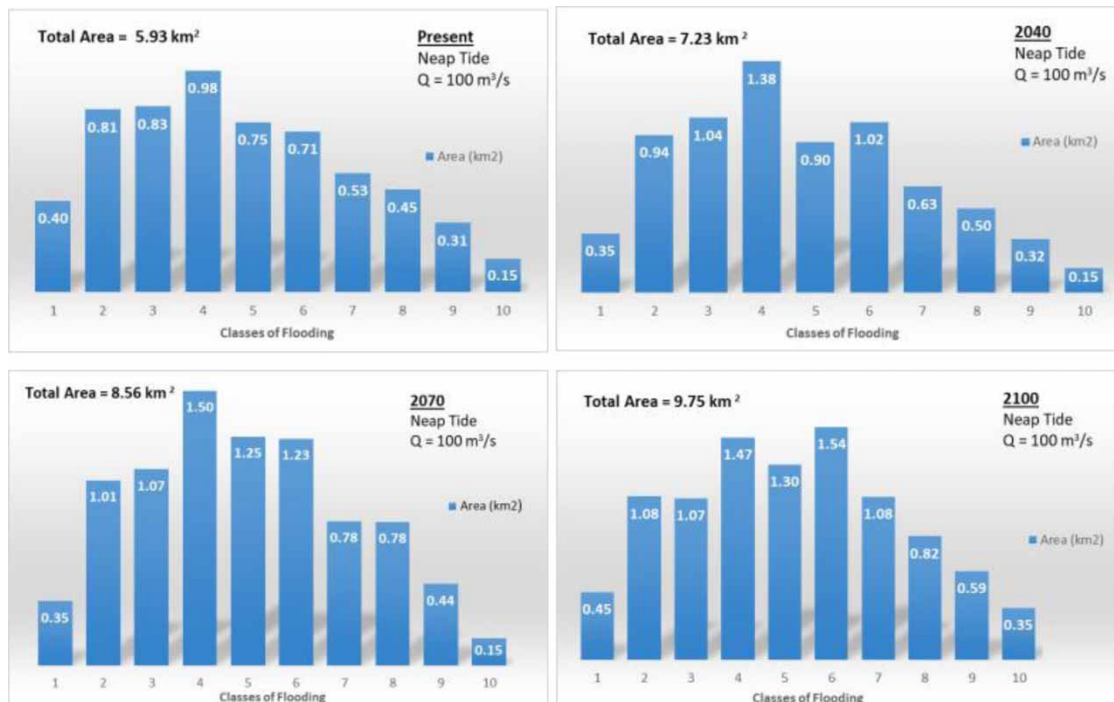


**Figure 14** | Histogram showing classes of flooding as a function of submersion time for one tidal cycle for the various scenarios of sea level rise at neap tide with a high freshwater flow.

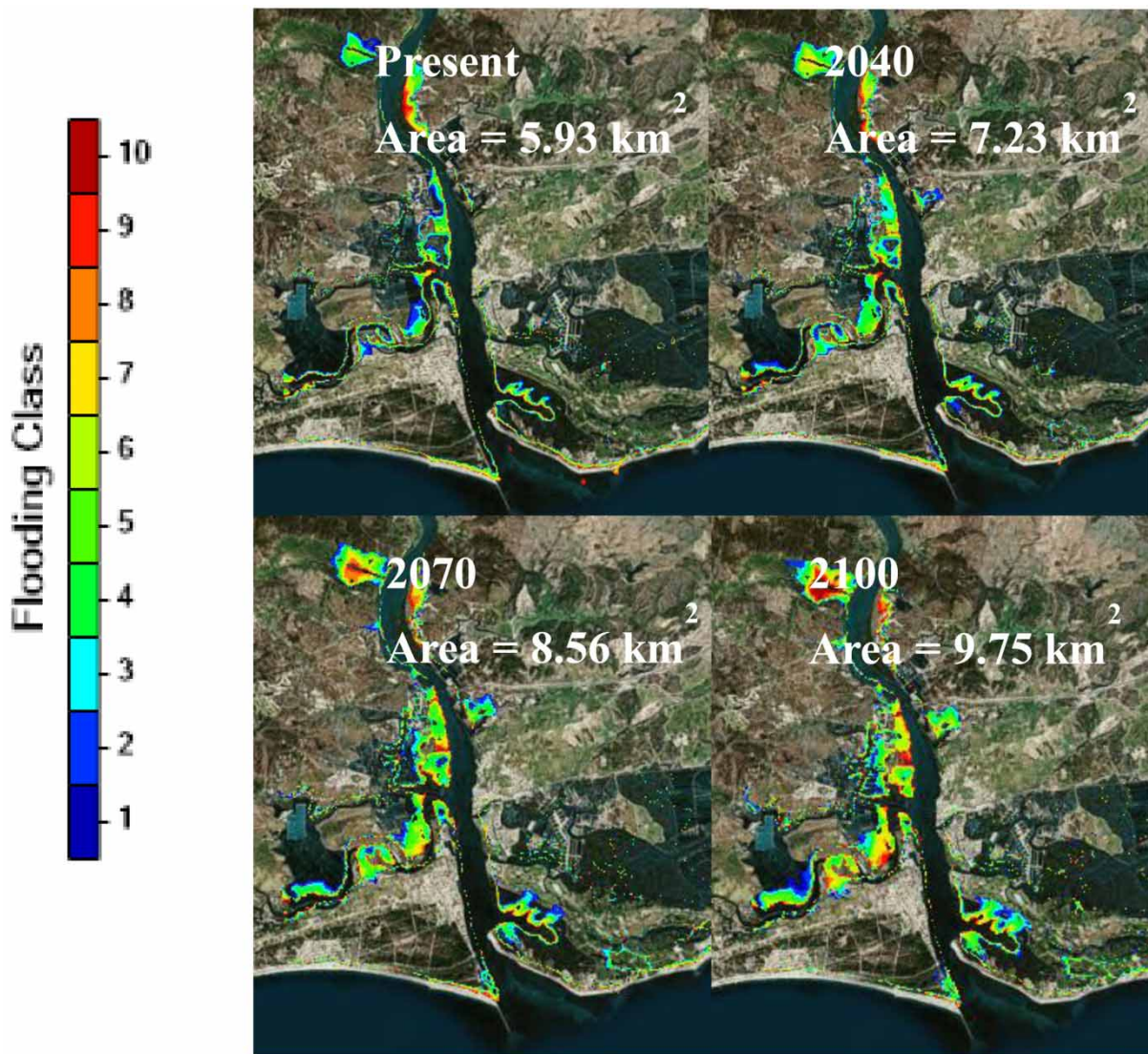


**Figure 15** | Flood distribution maps for a high freshwater discharge during neap tide for the various scenarios of sea level rise.

much further into the marshes, with some areas reaching salinity values close to 36 by 2100. Water velocity magnitude and direction also justify several of the salinity results. Especially for the present bathymetry, decreases in salinity coincide with decreases in water velocity. This result is attributed to the deepening of the channel from the increase in water volume, which has been known to occur in other shallow ebb-dominated estuaries (Friedrichs *et al.* 1990). Salinity increases with respect to mean sea level rise. Although the results from the present bathymetry may not portray an increase in salinity at the points chosen

for the time series, salinity does increase on the Spanish side of the estuary as shown in Figures 4 and 8. The bathymetry allowing flooding reveals a stronger correlation between sea level rise and salinity at each of the time series locations. Results obtained from this model are consistent with results from other numerical models which have found increases in estuarine salinity with respect to sea level rise (Hong & Shen 2012; Chua & Xu 2014; Vargas *et al.* 2017). The results of this model indicate that bathymetry, freshwater flow, and spring-neap tide variability impact the horizontal distribution of salinity intrusion caused by sea level rise.

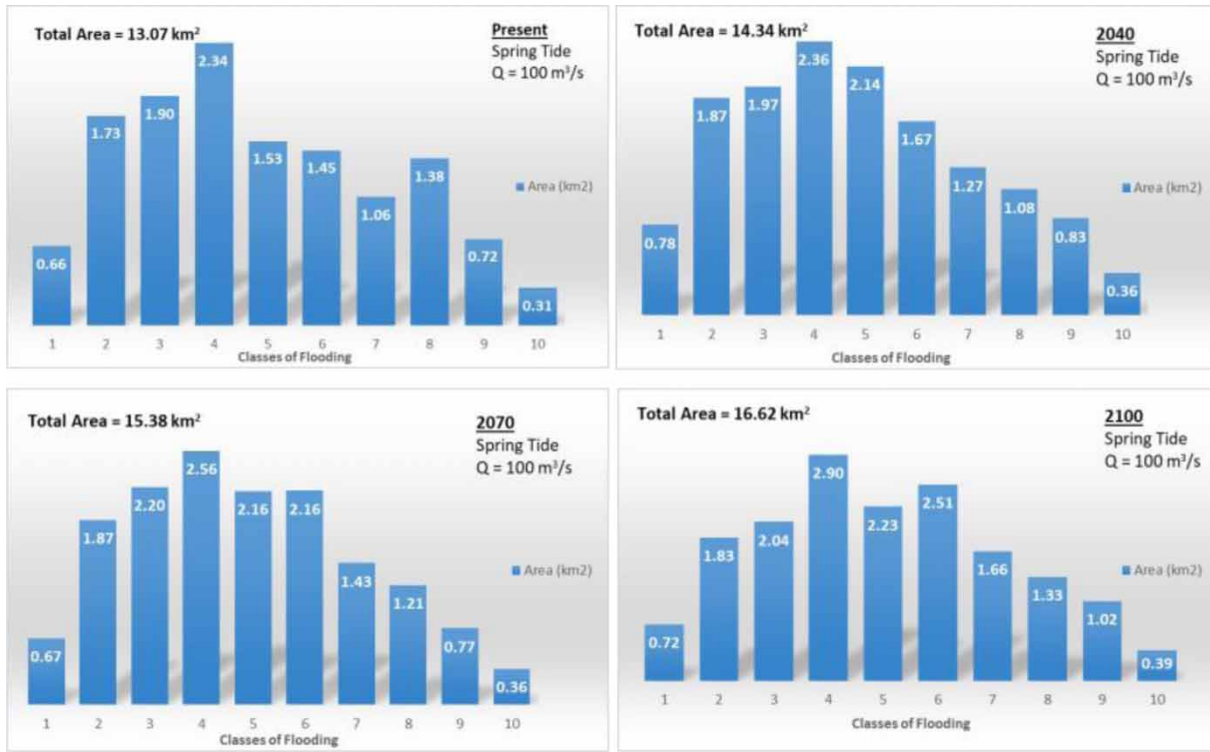


**Figure 16** | Histogram showing classes of flooding as a function of submersion time for one tidal cycle for the various scenarios of sea level rise at spring tide with a high freshwater flow.

Results from the salinity classes indicate that as sea level rises, a greater area of the Guadiana Estuary is covered by higher salinity values.

In terms of land inundation, all varying hydrodynamic factors result in an increase in inundation due to mean sea level rise. The area of inundation at neap tide is much smaller compared with the area of inundation at spring tide, which reflects how much sea level and tide contribute to the amount of land submerged. Furthermore, larger amounts of land are covered by higher flooding classes with respect to sea level rise.

## CONCLUSION

The two-dimensional MOHID water model produced maps demonstrating the hydrodynamics and salinity distribution to gain further insight into the future state of the Guadiana Estuary as it responds to climate change. The results of the

model demonstrate that the estuary responds differently to sea level rise based on freshwater flow, bathymetry, and tidal amplitude. All results portray an increase in salinity in response to sea level rise. The spatial distribution of salinity is dependent on the bathymetry as well as freshwater flow and tidal amplitude. When the freshwater flow is low in the spring and summer months, areas located upstream of the estuary increase in salinity. When the freshwater flow is high due to rainfall in the winter, the marshes west and east of the Guadiana Estuary in Portugal and Spain increase in salinity. A limitation of this work is the use of a two-dimensional model instead of a three-dimensional model. This was justified because the estuary is well-mixed, but there may be some variability in the water column due to the complex dynamics of the system, especially at neap tide. Additionally, a simple M2 tide was used, excluding the effects of overtides identified by [Garel & Cai \(2018\)](#) and [Quesada \*et al.\* \(2019\)](#). Future studies should use a three-dimensional model with real tidal signals

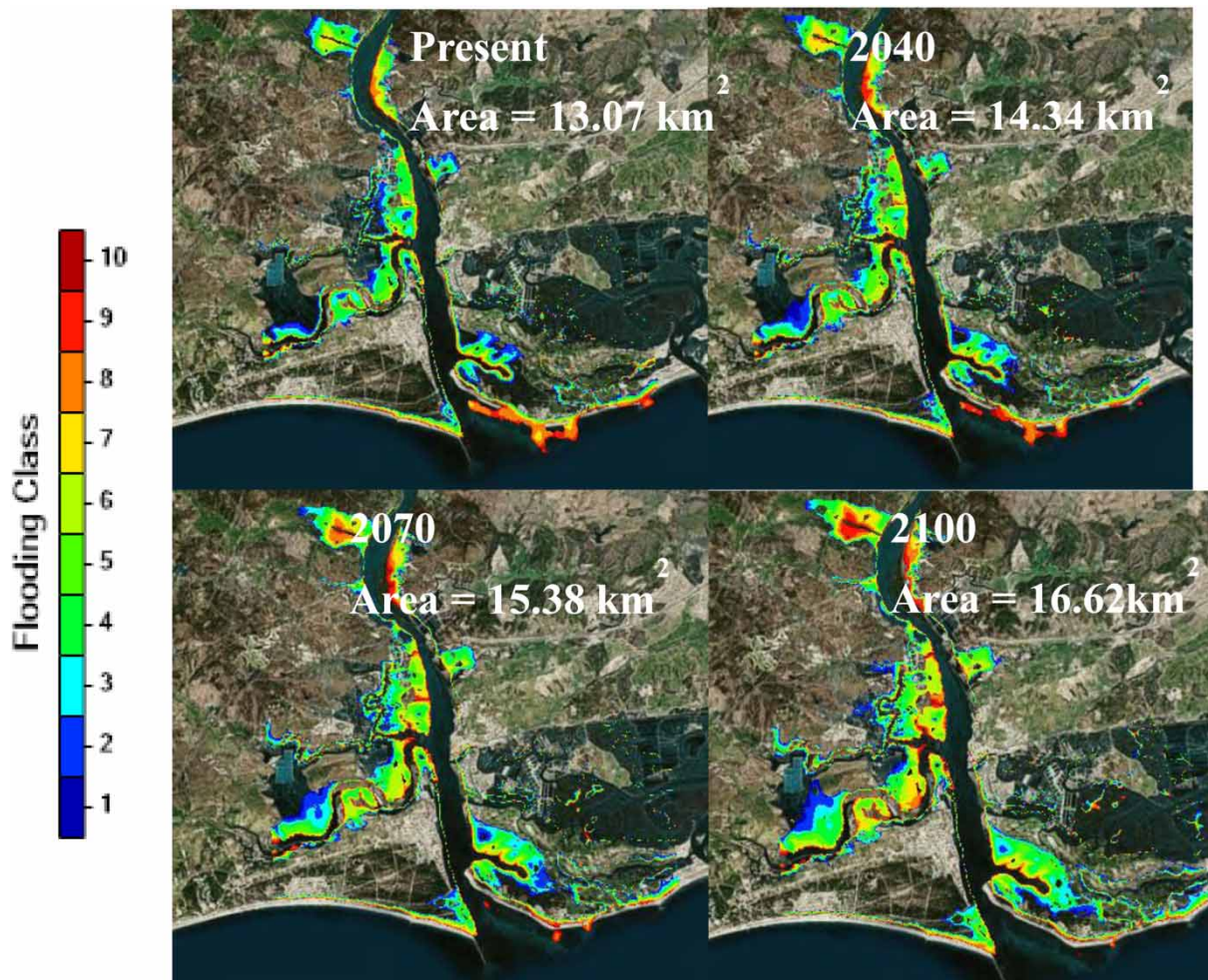


**Figure 17** | Flood distribution maps for a high freshwater discharge during spring tide for the various scenarios of sea level rise.

to allow for a more complete evaluation of the Guadiana Estuary and how it responds to climate change.

## DATA AVAILABILITY STATEMENT

All relevant data are included in the paper or its Supplementary Information.

## REFERENCES

- Basos, N. 2013 *GIS as a Tool to Aid Pre- and Post-Processing of Hydrodynamic Models. Application to the Guadiana Estuary*. Faculdade de Ciências e Tecnologia e Instituto Superior de Engenharia, Faro, Portugal.
- Carrasco, A. R., Ferreira, O. & Roelvink, D. 2016 *Coastal lagoons and rising sea level: a review*. *Earth-Science Reviews* **154**, 356–368. <https://doi.org/10.1016/j.earscirev.2015.11.007>.
- Chua, V. P. & Xu, M. 2014 *Impacts of sea-level rise on estuarine circulation: an idealized estuary and San Francisco Bay*. *Journal of Marine Systems* **139**, 58–67. <https://doi.org/10.1016/j.jmarsys.2014.05.012>.
- Church, J. A., Clark, P. U., Cazenave, A., Gregory, J. M., Jevrejeva, S., Levermann, A. & Unnikrishnan, A. S. 2013 Sea level change. In: *Climate Change 2013: The Physical Science Basis. Contribution of Working Group I to the Fifth Assessment Report of the Intergovernmental Panel on Climate Change*, pp. 1137–1216. <https://doi.org/10.1017/CB09781107415315.026>.

- Delgado, J., Boski, T., Nieto, J. M., Pereira, L., Moura, D., Gomes, A. & García-Tenorio, R. 2012 *Sea-level rise and anthropogenic activities recorded in the late Pleistocene/Holocene sedimentary infill of the Guadiana Estuary (SW Iberia)*. *Quaternary Science Reviews* **33**, 121–141. <https://doi.org/10.1016/j.quascirev.2011.12.002>.
- Fortunato, A. B., Oliveira, A. & Alves, E. T. 2002 Circulation and salinity intrusion in the Guadiana Estuary (Portugal/Spain). *Thalassas* **18** (2), 43–65.
- Friedrichs, C. T., Aubrey, D. G. & Speer, P. K. 1990 Impacts of relative sea-level rise on evolution of shallow estuaries. In: *Residual Currents and Long-Term Transport. Coastal and Estuarine Studies* (R. T. Cheng, ed.). Springer, New York, pp. 106–122.
- Garel, E. & Cai, H. 2018 *Effects of tidal-forcing variations on tidal properties along a narrow convergent estuary*. *Estuaries and Coasts* **41** (7), 1924–1942. <https://doi.org/10.1007/s12237-018-0410-y>.
- Garel, E. & D'Alimonte, D. 2017 *Continuous river discharge monitoring with bottom-mounted current profilers at narrow tidal estuaries*. *Continental Shelf Research* **133**, 1–12. <https://doi.org/10.1016/j.csr.2016.12.001>.
- Garel, E., Pinto, L., Santos, A. & Ferreira, Ó. 2009 *Tidal and river discharge forcing upon water and sediment circulation at a rock-bound estuary (Guadiana Estuary, Portugal)*. *Estuarine, Coastal and Shelf Science* **84** (2), 269–281. <https://doi.org/10.1016/j.ecss.2009.07.002>.
- Hong, B. & Shen, J. 2012 *Responses of estuarine salinity and transport processes to potential future sea-level rise in the Chesapeake Bay*. *Estuarine, Coastal and Shelf Science* **104–105**, 33–45. <https://doi.org/10.1016/j.ecss.2012.03.014>.
- Lopes, J., Neves, R., Dias, J. M. A. & Martins, F. 2003 Calibração De Um Sistema De Modelação Para O Estuário Do. In *4th Symposium on the Iberian Atlantic Margin*, pp. 4–6.
- MARETEC 2017 *MOHID Water*. Available from: [http://wiki.mohid.com/index.php?title=Mohid\\_Water](http://wiki.mohid.com/index.php?title=Mohid_Water) (retrieved 4 April 2019).
- McLean, R. F., Tsyban, A., Burkett, V., Codignott, J. O., Forbes, D. L., Mimura, N., Beamish, R. J. & Ittekkot, V. 2001 Coastal zones and marine ecosystems. In: *Climate Change 2001: Impacts, Adaptation, and Vulnerability. Contribution of Working Group II to the Third Assessment Report of the Intergovernmental Panel on Climate Change* (J. J. McCarthy, O. F. Canziani, N. A. Leary, D. J. Dokken & K. S. White, eds). Cambridge University Press, Cambridge, pp. 343–379.
- Mills, L., Janeiro, J. & Martins, F. 2019 The impact of sea level rise in the Guadiana Estuary. In: *Computational Science – ICCS 2019. ICCS 2019. Lecture Notes in Computer Science*, Vol. 11539 (R. J. Cardoso, J. Monteiro, R. Lam, V. Krzhizhanovskaya, M. Lees, J. Dongarra & P. Sloot, eds). pp. 287–300. [https://doi.org/10.1007/978-3-030-22747-0\\_23](https://doi.org/10.1007/978-3-030-22747-0_23).
- Morais, P., Martins, F., Chicharro, M. A., Lopes, J. & Chicharro, L. 2012 *Merging anchovy eggs abundance into a hydrodynamic model as an assessment tool for estuarine ecohydrological management*. *River Research and Applications* **28** (2), 160–176. <https://doi.org/10.1002/rra.1443>.
- Neves, R., Silva, A., Delfino, J., Leitão, P., Leitão, J., Pina, P. & Coelho, H. 2000 Coastal management supported by modelling: optimising the level of treatment of urban discharges into coastal waters. *Environmental Studies* **5**, 41–49.
- Nicholls, R. J., Marinova, N., Lowe, J. A., Brown, S., Vellinga, P., De Gusmão, D. & Tol, R. S. J. 2011 *Sea-level rise and its possible impacts given a 'beyond 4°C world' in the twenty-first century*. *Philosophical Transactions of the Royal Society A: Mathematical, Physical and Engineering Sciences* **369** (1934), 161–181. <https://doi.org/10.1098/rsta.2010.0291>.
- Oliveira, A., Fortunato, A. B. & Pinto, L. 2006 *Modelling the hydrodynamics and the fate of passive and active organisms in the Guadiana Estuary*. *Estuarine, Coastal and Shelf Science* **70** (1–2), 76–84. <https://doi.org/10.1016/j.ecss.2006.05.033>.
- Quesada, M. C. C., García-Lafuente, J., Garel, E., Delgado Cabello, J., Martins, F. & Moreno-Navas, J. 2019 *Effects of tidal and river discharge forcings on tidal propagation along the Guadiana Estuary*. *Journal of Sea Research* **146**, 1–13. <https://doi.org/10.1016/j.seares.2019.01.006>.
- Sampath, D. M. R. & Boski, T. 2016 *Morphological response of the saltmarsh habitats of the Guadiana Estuary due to flow regulation and sea-level rise*. *Estuarine, Coastal and Shelf Science* **183**, 314–326. <https://doi.org/10.1016/j.ecss.2016.07.009>.
- Sampath, D. M. R., Boski, T., Silva, P. L. & Martins, F. A. 2011 *Morphological evolution of the Guadiana Estuary and intertidal zone in response to projected sea-level rise and sediment supply scenarios*. *Journal of Quaternary Science* **26** (2), 156–170. <https://doi.org/10.1002/jqs.1434>.
- Sampath, D. M. R., Boski, T., Loureiro, C. & Sousa, C. 2015 *Modelling of estuarine response to sea-level rise during the Holocene: application to the Guadiana Estuary-SW Iberia*. *Geomorphology* **232**, 47–64. <https://doi.org/10.1016/j.geomorph.2014.12.037>.
- Vargas, C. I. C., Vaz, N. & Dias, J. M. 2017 *An evaluation of climate change effects in estuarine salinity patterns: application to Ria de Aveiro shallow water system*. *Estuarine, Coastal and Shelf Science* **189**, 33–45. <https://doi.org/10.1016/j.ecss.2017.03.001>.

First received 6 July 2020; accepted in revised form 15 February 2021. Available online 12 March 2021